Phys. Status Solidi B **249,** No. 8, 1541–1545 (2012) / **DOI** 10.1002/pssb.201248064

physica status solidi b
www.pss-b.com
basic solid state physics

Solid-state formation of ferromagnetic δ-$Mn_{0.6}Ga_{0.4}$ thin films with high rotatable uniaxial anisotropy

V. G. Myagkov[*,1,2], V. S. Zhigalov[1,2], L. E. Bykova[1], G. N. Bondarenko[3], Yu. L. Mikhlin[3], G. S. Patrin[1,4], and D. A. Velikanov[1,4]

[1] Kirensky Institute of Physics, Russian Academy of Sciences, Siberian Branch, Krasnoyarsk 660036, Russia
[2] Reshetnev Siberian State Aerospace University, Krasnoyarsk 660014, Russia
[3] Institute of Chemistry and Chemical Technology, Russian Academy of Sciences, Siberian Branch, Krasnoyarsk 660049, Russia
[4] Siberian Federal University, Krasnoyarsk 660041, Russia

Received 17 January 2012, revised 16 March 2012, accepted 21 March 2012
Published online 18 April 2012

Keywords high anisotropy constants, Mn_xGa_{1-x} alloys, rotatable magnetic anisotropies, thin films

[*] Corresponding author: e-mail miagkov@iph.krasn.ru, Phone: +7 391 2494681, Fax: +7 391 2438923

Solid-state reactions in Ga/Mn polycrystalline films of the composition 1 Ga:3 Mn were experimentally investigated. Our X-ray study showed that the formation of the Ga/Mn → (250 °C) ϕ-$Ga_{7.7}Mn_{2.3}$ → (350 °C) δ-$Mn_{0.6}Ga_{0.4}$ phase sequence occurs when the annealing temperature is increased to 400 °C. δ-$Mn_{0.6}Ga_{0.4}$ samples were found to have high rotatable uniaxial anisotropy. We also showed that magnetic fields with coercivities above $H > H_C = 8.3$ kOe can be used to orient the easy anisotropy axis in any spatial direction while taking the angle of the lag into account.

1 Introduction Films of Mn_xGa_{1-x} alloys have attracted a great deal of attention because of their high spin polarization, large perpendicular magnetic anisotropy (PMA), low magnetization, high Curie temperature, and good hysteresis properties [1–10]. The phase equilibrium diagrams for Ga–Mn systems in areas rich in Mn have a thermodynamically stable ferromagnetic tetragonal δ-$Mn_{0.6}Ga_{0.4}$ phase [1–6], metastable tetragonal ferrimagnetic $Mn_{3-\delta}Ga$ phases with DO_{22} structures [7–9], and a ferromagnetic quasi-crystal phase [10]. Depending on the composition and annealing conditions, these phases have coercivities in the range $H_C = (2–10)$ kOe and saturation magnetizations between $M_S = (250–450)$ emu/cm^3. In tetragonal δ-$Mn_{0.6}Ga_{0.4}$ and $Mn_{3-\delta}Ga$ alloys, the easy magnetization direction coincides with the *c*-axis. Epitaxial (001) films of these alloys deposited onto GaAs(001) and MgO(001) substrates are characterized by high PMA. Namely, they have large values for the first constant of the magnetocrystallographic anisotropy (K_1) of the δ-$Mn_{0.6}Ga_{0.4}$ and $Mn_{3-\delta}Ga$ phases. Therefore, the Mn_xGa_{1-x} films are promising for spintronic applications [11].

Studies of thermodynamic stability of the Mn/GaAs(001), Mn/GaN(001), and Mn/GaP(001) thin films have shown that, with increasing annealing temperature, synthesis of Mn_2As, MnAs, and MnP occurs and both epitaxial and polycrystalline Mn_xGa_{1-x} clusters are formed [12–16]. The same synthesis products can be obtained via implantation of Mn ions in GaAs [17] and GaN [18, 19] substrates.

The nature of high-temperature ferromagnetism in diluted semiconductors has not been fully explained. One of the possible explanations is the formation of ferromagnetic nanoclusters because of chemical phase separation. In particular, ferromagnetic Mn_xGa_{1-x} and MnAs nanoclusters have been observed in (Ga, Mn)As solid solutions after high-temperature annealing and were attributed to spinodal decomposition [20–24]. The parameters and mechanisms of the chemical interaction between Mn and semiconductor substrates is still not well understood. To investigate the formation of Mn-based magnetic phases, it is necessary to study the typical behavior of the solid-state reactions among Mn, Ga, As, N, and P.

In this work, we investigate the sequence of phase formation in Ga/Mn film samples with the composition 1Ga:3Mn. We work with annealing temperatures as high as 400 °C. We demonstrate the formation of the

Ga/Mn → (250 °C) ϕ-$Ga_{7.7}Mn_{2.}$ → (350 °C) δ-$Mn_{0.6}Ga_{0.4}$ phase sequence and present the magnetic characteristics of the reaction products. Also, we discuss the possibility that the formation of magnetic Mn_xGa_{1-x} phases at the interface between the Mn and semiconductor substrates may occur upon phase separation in the diluted semiconductors.

2 Experimental details The initial Ga/Mn film structures were prepared via the successive thermal deposition of Mn and Ga layers onto glass substrates in vacuum at a residual pressure of 10^{-6} mbar. In the experiments, we used samples with the atomic ratio 1Ga:3Mn and a total thickness of 400 nm. The manganese layers were deposited at temperatures between 220 and 250 °C. The gallium layers were deposited at room temperature to avoid solid-state reactions between the Ga and Mn during deposition. The obtained Ga/Mn samples were annealed at temperatures between 50 and 400 °C at 50 °C intervals. The samples were held at each temperature for 30 min. The saturation magnetization M_S was measured on an MPMS-XL SQUID magnetometer (Quantum Design) in magnetic fields as high as 50 kOe. The magnetic anisotropy was studied using a torque magnetometer with a sensitivity of 3.76×10^{-3} dyn/cm. The forming phases were identified by X-ray diffraction with Cu Kα radiation. The thicknesses of the Ga and Mn layers were determined via X-ray fluorescent analysis. All of the measurements were performed at room temperature.

3 Results and discussion The initial Ga/Mn samples remained nonmagnetic for annealing temperatures below 250 °C. After annealing at 300 °C, minor magnetization was found. The magnitude of the magnetization grew drastically after annealing at 400 °C. The occurrence of magnetization at 250 °C and its sharp growth at 350 °C indicate that intermixing occurred between the Ga and Mn layers. Moreover, it suggests that the solid-state synthesis of two magnetic phases (with initiation temperatures $T_0^1 \sim 250$ °C and $T_0^2 \sim 350$ °C, respectively), occurred in the samples. The diffraction patterns for the initial Ga/Mn films (Fig. 1a) contained weak responses for α-Mn and metastable β-Ga phase. The formation of the β-Ga phase and other metastable polymorphous modifications of Ga are related to undercooling phenomena [25] or size effect [26]. After annealing at 300 °C, the responses from Ga and Mn vanished and features corresponding to a cubic ϕ-$Ga_{7.7}Mn_{2.3}$ phase developed (Fig. 1b). For an annealing temperature of 350 °C, responses corresponding to a δ-$Mn_{0.6}Ga_{0.4}$ phase with the lattice parameters $a = 0.2753$ nm and $b = 0.3638$ nm were observed. These peaks dominated after annealing at 400 °C (Fig. 1c). However, additional weak responses, which can be attributed to manganese carbides and oxides, were also observed in the diffraction patterns after annealing at 400 °C. These results indicate that formation of a Ga/Mn → (250 °C)ϕ-$Ga_{7.7}Mn_{2.3}$ → (350 °C)δ-$Mn_{0.6}Ga_{0.4}$ phase sequence in the Ga/Mn samples occurs after annealing at 400 °C.

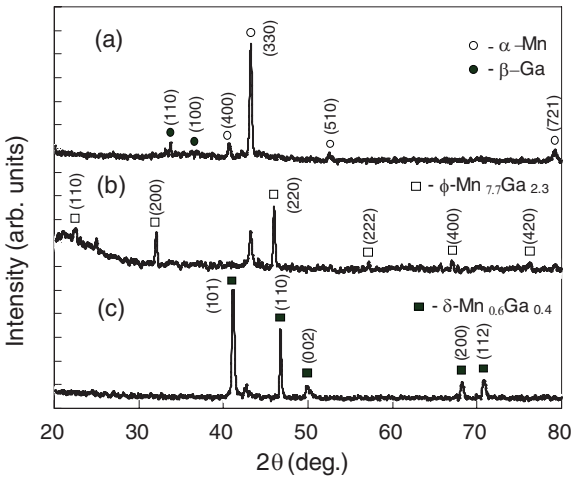

Figure 1 Diffraction patterns for the Ga/Mn film system: (a) initial sample, and sample after annealing at (b) 250 °C and (c) 400 °C.

Figure 2 shows both in-plane and perpendicular hysteresis loops (M–H) for the δ-$Mn_{0.6}Ga_{0.4}$ sample that was annealed at 400 °C. The loops for both cases are similar and the magnetization does not saturate even when the sample is exposed to a magnetic field of 50 kOe. The magnetization ($M_S = 360$ emu/cm^3) at 50 kOe is similar to the values for saturation in bulk and film samples with this phase [1–6]. The fact that the in-plane and perpendicular hysteresis loops for the sample are the same and the coercivity value $H_C \sim 8.3$ kOe is invariable imply that the δ-$Mn_{0.6}Ga_{0.4}$ crystallites are randomly oriented in the film sample. The torque curves in the film plane $L_{||}(\varphi)$ demonstrate the high uniaxial anisotropy of the sample. The easy axis rotates along with the high magnetic field. Figure 3 shows the $L_{||}(\varphi)$ curves

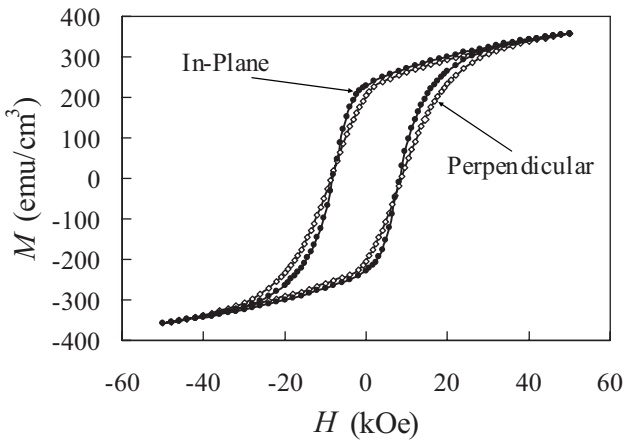

Figure 2 Magnetization curves (M–H) for the polycrystalline δ-$Mn_{0.6}Ga_{0.4}$ film for the magnetic field (H) applied parallel (filled circles) and perpendicular (empty diamonds) to the film plane. Similar hysteresis loops can be explained by the formation δ-$Mn_{0.6}Ga_{0.4}$ crystallites randomly oriented by the c-axis with the high rotatable uniaxial anisotropy considerably exceeding the shape anisotropy.

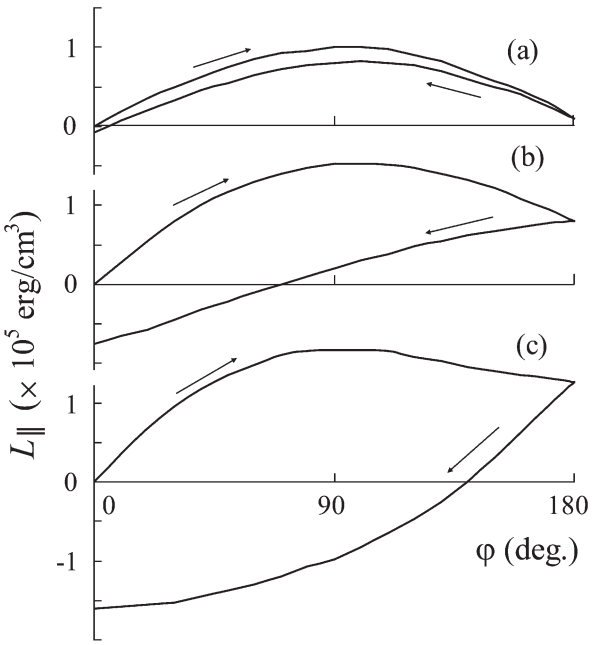

Figure 3 Torque curves $L_{||}(\varphi)$ in the plane of the δ-$Mn_{0.6}Ga_{0.4}$ film sample for increasing values of magnetic field H: (a) 6 kOe, (b) 10 kOe, and (c) 14 kOe. For the fields in which $H > H_C = 8.3$ kOe, the easy axis of the uniaxial anisotropy rotates. Similar curves for $L_{\perp}(\varphi)$ are obtained through the rotation of the H field in the plane through the film normal in the opposite direction.

for the magnetic field (H) as it rotates $\varphi = 180^\circ$ clockwise (forward trace) and counterclockwise (backward trace) in the sample plane about the easy axis. In low fields ($H_C > H = 6$ kOe), the forward and backward traces are similar, and the easy magnetization direction does not change. The high hysteresis between the forward and backward trace curves for fields of $H = 10$ and 14 kOe occurs because of the presence of the rotatable anisotropy in the δ-$Mn_{0.6}Ga_{0.4}$ sample. Specifically, for fields of $H = 10$ and 14 kOe, the easy axis rotates by angles of 70° and 140°, respectively (Fig. 3). The curves for the torques perpendicular to the film plane $L_{\perp}(\varphi)$ from the easy axis direction to the normal of the opposite direction are analogous. The equivalence of the torque curves in the film plane $L_{||}(\varphi)$ and perpendicular to the film plane $L_{\perp}(\varphi)$ implies that for fields in which $H > H_C = 8.3$ kOe, if the angle of lag is taken into account, the easy axis can be oriented in any direction. These results are consistent with the measurements of the hysteresis loops (Fig. 2) and confirm the spatial isotropy of the magnetic properties. This isotropy is related to the random orientation of the δ-$Mn_{0.6}Ga_{0.4}$ crystallites. The numerical values for the torques $L_{\perp}(\varphi)$ and $L_{||}(\varphi)$ are similar. This means that the shape anisotropy is small compared with the uniaxial anisotropy constant (K_U). The exact value of K_U is difficult to estimate. Assuming that there is no self-interaction among the δ-$Mnn_{0.6}Ga_{0.4}$ crystallites, the Stoner–Wohlfarth [27] model for single-domain particles allows for a rough estimate of the constant: $K_U = M_S \times H_C/0.958 = 3.1 \times 10^6$ erg/cm^3. This value is smaller than the PMA constant for epitaxial $Mn_{2.5}Ga$ films but only by a factor of 4 [7]. This suggests that the large value of the uniaxial anisotropy constant in the samples is determined by the first constant of the magnetocrystallographic anisotropy of the δ-$Mn_{0.6}Ga_{0.4}$ phase.

Although, the fundamental mechanisms guiding the rotatable anisotropy are not well understood, it can be explained by the exchange interaction at the antiferromagnet/ferromagnet interface. Specifically, rotatable anisotropy was observed in exchange-coupled Ni/NiO [28], Co/CoO [29], and Fe/$KNiF_3$ [30] bilayers. The X-ray photoelectron spectra of the surface of the initial and reacted films contained oxygen and carbon lines. We propose that, in the deposition and annealing processes described above, manganese oxides and carbides are formed. The Curie temperatures of manganese oxides are below room temperature. However, metastable MnC [31], Mn_2C, Mn_3C, Mn_5C_2, and $Mn_{23}C_6$ [32] carbides can be ferromagnetic or antiferromagnetic at room temperature. Moreover, these compounds may play an important role in the observed rotatable anisotropy.

A possible, alternative, explanation of the existence of rotational anisotropy may consist the following. During the solid-state synthesis, exchange-coupled δ-$Mn_{0.6}Ga_{0.4}$ crystallites with randomly oriented ***c***-axes are formed. Under the action of a high magnetic field, $H \gg H_C$, magnetizations of the crystallites are arranged along the c-axes in the direction coinciding with the direction of the field and form a common easy magnetization axis. Therefore, in small fields, $H < H_C = 8.3$ kOe, the curves of the moments are described by the law $L \sim \sin\varphi$ (Fig. 3). In the fields $H > H_C = 8.3$ kOe, rotation of the magnetic field from the direction of the common easy axis leads to magnetization reversal of the crystallites with the c-axes close to the field direction. This causes rotation of the common easy axis and creates the rotational anisotropy effect.

Values of the in-plane rotational anisotropy for different metals and alloys are insignificant, the highest value of the anisotropy constant $K_U \sim 1 \times 10^6$ erg/g was found in Tb–Fe alloys [33]. Important features of the investigated δ-$Mn_{0.6}Ga_{0.4}$ samples are high values of H_C and K_U and the existence of the rotational anisotropy, both in the film plane and perpendicular to it.

In this study [34], the solid-state synthesis of magnetically soft ϕ-$Ga_{7.7}Mn_{2.3}$ phase in 1Mn:3Ga Ga/Mn bilayers was investigated. The magnetic and structural characteristics of this phase were reported. The initiation temperature of the ϕ-$Ga_{7.7}Mn_{2.3}$ phase was 250 °C. The phase remained in the sample after annealing at 400 °C. Also, in the 1Ga:3Mn Ga/Mn bilayer films, the ϕ-$Ga_{7.7}Mn_{2.3}$ phase first forms at the Ga/Mn interface at 250 °C. However, at 350 °C, a solid-state reaction between the residual Mn and ϕ-$Ga_{7.7}Mn_{2.3}$ layers occurs, which results in the formation of a magnetically hard δ-$Mn_{0.6}Ga_{0.4}$ phase that is rich in Mn.

Numerous investigations show that in bilayer and multilayer films heated up to a certain temperature (initiation

temperature T_0), a phase of reaction products forms. This phase is named the first phase. With further increase in the annealing temperature, new phases sequentially form, creating a phase sequence. The initiation temperatures of the phases are universal characteristics of solid-state reactions for a given binary system. They do not depend on the way film reagents are deposited and morphology and weakly depend on contamination of the interface. The formation of the only first phase among various equilibrium phases and of the phase sequence is a unique, unexplained phenomenon of the solid-state synthesis of film materials. A number of attempts were made to predict the formation of the first phase. They were based, as a rule, on consideration of a high-temperature portion of the state diagram or on thermodynamic arguments. However, by now no commonly accepted suggestions concerning the formation of the first phase, the phase sequence, and the initiation temperatures have been made [35–38].

We are confident that the chemical interaction between elemental Ga and Mn can be the basis of not only the solid-state synthesis of the ϕ-$Ga_{7.7}Mn_{2.3}$ and δ-$Mn_{0.6}Ga_{0.4}$ phases in the Ga/Mn films, but also the formation of Mn_xGa_{1-x} nanoclusters in Mn/GaAs and Mn/GaSb samples and, upon low-temperature spinodal decomposition, in (Ga, Mn)As films. Note that the initiation temperature of the δ-$Mn_{0.6}Ga_{0.4}$ phase in the Ga/Mn films ($\tau_0 \sim 350\,^{\circ}C$) reported in this work is similar to the initiation temperature of this same phase in Mn/GaAs [12, 13]. This suggests that the initiation temperatures and chemical mechanisms for the synthesis of δ-$Mn_{0.6}Ga_{0.4}$ are similar in both cases. Therefore, one should expect that the formation of the first ϕ-$Ga_{7.7}Mn_{2.3}$ phase (at $\sim$250 °C in the Mn/GaAs samples) will occur prior to the formation of δ-$Mn_{0.6}Ga_{0.4}$. This is in agreement with a previous study that showed that ϕ-$Ga_{7.7}Mn_{2.3}$ was the first phase to form at the Mn/GaSb interface [39].

As the annealing temperature increases, most diluted magnetic semiconductors undergo spinodal decomposition, which may explain the occurrence of ferromagnetic ordering at room temperature. However, the components and initiation temperatures for phase separations are hard to measure experimentally [20, 21]. Coherent Mn(Ga)As nanoclusters rich in manganese and embedded in GaAs can be formed by annealing (Ga, Mn)As films at high temperatures (above 500 °C) [23]. However, MnAs precipitates begin growing at 260 °C [24]. The results of this study suggest that the strong chemical interactions among Mn, Ga, Mn, As, N, and P may be the basis for the spinodal decomposition. Therefore, at temperatures of $\sim$250 and $\sim$350 °C, one may expect to observe the formation of ferromagnetic ϕ-$Ga_{7.7}Mn_{2.3}$ and δ-$Mn_{0.6}Ga_{0.4}$ precipitates in (Ga, Mn)As, (Ga, Mn)N, and (Ga, Mn)P diluted semiconductors.

4 Conclusions Thus, we have investigated phase transformations in polycrystalline Ga/Mn nanofilms with the composition 1Ga:3Mn for annealing temperature as high as 400 °C. The magnetically soft ϕ-$Ga_{7.7}Mn_{2.3}$ and magnetically hard δ-$Mn_{0.6}Ga_{0.4}$ phases form at $\sim$250 and $\sim$350 °C, respectively. The easy axis of the strong uniaxial anisotropy of the δ-$Mn_{0.6}Ga_{0.4}$ samples can be rotated both in-plane and perpendicularly using fields with coercivities above H_C. The simple synthesis techniques, high uniaxial anisotropy, and controllable easy-axis direction of the polycrystalline ϕ-$Ga_{7.7}Mn_{2.3}$ and δ-$Mn_{0.6}Ga_{0.4}$ films allow for the use of these films in a large number of practical applications.

References

[1] K. M. Krishnan, Appl. Phys. Lett. **61**, 2365 (1992).
[2] M. Tanaka, J. P. Harbison, J. DeBoeck, T. Sands, B. Philips, T. L. Cheeks, and V. G. Keramidas, Appl. Phys. Lett. **62**, 1565 (1993).
[3] C. Adelmann, J. L. Hilton, B. D. Schultz, S. McKernan, C. J. Palmstrøm, X. Lou, H.-S. Chiang, and P. A. Crowell, Appl. Phys. Lett. **89**, 112511 (2006).
[4] K. Wang, A. Chinchore, W. Lin, D. C. Ingram, A. R. Smith, A. J. Hauser, and F. Yang, J. Cryst. Growth **311**, 2265 (2009).
[5] K. Wang, E. Lu, J. W. Knepper, F. Yang, and A. R. Smith, Appl. Phys. Lett. **98**, 162507 (2011).
[6] S. Mizukami, T. Kubota, F. Wu, X. Zhang, T. Miyazaki, H. Naganuma, M. Oogane, A. Sakuma, and Y. Ando, Phys. Rev. B **85**, 014416 (2012).
[7] F. Wu, E. P. Sajitha, S. Mizukami, D. Watanabe, T. Miyazaki, H. Naganuma, M. Oogane, and Y. Ando, Appl. Phys. Lett. **96**, 042505 (2010).
[8] W. Feng, D. V. Thiet, D. D. Dung, Y. Shin, and S. Cho, J. Appl. Phys. **108**, 113903 (2010).
[9] H. Kurt, K. Rode, M. Venkatesan, P. Stamenov, and J. M. D. Coey, Phys. Rev. B **83**, 020405 (R) (2011).
[10] J. P. Zhang, A. K. Cheetham, K. Sun, J. S. Wu, K. H. Kuo, J. Shi, and D. D. Awschalom, Appl. Phys. Lett. **71**, 143 (1997).
[11] S. Mangin, D. Ravelosona, J. A. Katine, M. J. Carey, B. D. Terris, and E. E. Fullerton, Nature Mater. **5**, 210 (2006).
[12] J. L. Hilton, B. D. Schultz, S. McKernan, and C. J. Palmstrom, Appl. Phys. Lett. **84**, 3145 (2004).
[13] J. L. Hilton, B. D. Schultz, and C. J. Palmstrom, J. Appl. Phys. **102**, 063513 (2007).
[14] A. Chanda, H. P. Lenka, and C. Jacob, J. Supercond. Novel Magn. **22**, 401 (2009).
[15] Y. Osafune, G. S. Song, J. I. Hwang, Y. Ishida, M. Kobayashi, K. Ebata, Y. Ooki, A. Fujimori, J. Okabayashi, K. Kanai, K. Kubo, and M. Oshima, J. Appl. Phys. **103**, 103717 (2008).
[16] I. G. Bucsa, R. W. Cochrane, and S. Roorda, J. Appl. Phys. **106**, 013914 (2009).
[17] O. D. D. Couto, M. J. S. P. Brasil, F. Iikawa, C. Giles, C. Adriano, J. R. R. Bortoleto, M. A. A. Pudenzi, H. R. Gutierrez, and I. Danilov, Appl. Phys. Lett. **86**, 071906 (2005).
[18] L. Sun, F. Yan, J. Wang, Y. Zeng, G. Wang, and J. Li, Phys. Status Solidi A **206**, 91 (2009).
[19] J. M. Baik, H. S. Kim, C. G. Park, and J.-L. Lee, Appl. Phys. Lett. **83**, 2632 (2003).
[20] A. Bonanni and T. Dietl, Chem. Soc. Rev. **39**, 528 (2010).
[21] T. Dietl, Nature Mater. **9**, 965 (2010).
[22] P. N. Hai, S. Yada, and M. Tanaka, J. Appl. Phys. **109**, 073919 (2011).

[23] W. Z. Wang, J. J. Deng, J. Lu, B. Q. Sun, X. G. Wu, and J. H. Zhao, J. Appl. Phys. **105**, 053912 (2009).
[24] T. Hayashi, Y. Hashimoto, S. Katsumoto, and Y. Iye, Appl. Phys. Lett. **78**, 1691 (2001).
[25] E. A. Sutter, P. W. Sutter, E. Uccelli, and A. F. i Morral, Phys. Rev. B **84**, 193303 (2011).
[26] H. He, G. Tao Fei, P. Cui, K. Zheng, L. M. Liang, Y. Li, and L. D. Zhang, Phys. Rev. B **72**, 073310 (2005).
[27] E. C. Stoner and E. P. Wohlfarth, Philos. Trans. R. Soc. Lond., Ser. A **240**, 599 (1948).
[28] J. M. Lommel and J. C. D. Graham, J. Appl. Phys. **33**, 1160 (1962).
[29] T. Gredig, I. N. Krivorotov, and E. Dan Dahlberg, Phys. Rev. B **74**, 094431 (2006).
[30] L. Wee, R. L. Stamps, L. Malkinski, and Z. Celinski, Phys. Rev. B **69**, 134426 (2004).
[31] J. J. Hauser, Phys. Rev. B **22**, 2554 (1980).
[32] D. Djurovic, B. Hallstedt, J. von Appen, and R. Dronskowski, Calphad **34**, 279 (2010).
[33] M. J. O'Shea, K. M. Lee, and A. Fert, J. Appl. Phys. **67**, 5769 (1990).
[34] V. G. Myagkov, V. S. Zhigalov, L. E. Bykova, L. A. Solov'ev, G. S. Patrin, and D. A. Velikanov, JETP Lett. **92**, 687 (2010).
[35] J. M. Poate, K. N. Tu, and J. W. Mayer (eds.), Thin Films – Interdiffusion and Reaction (Wiley-Interscience, New York, 1978).
[36] E. G. Colgan, Mater. Sci. Rep. **5**, 1 (1990).
[37] R. Pretorius, C. C. Theron, A. Vantomme, and J. W. Mayer, Crit. Rev. Solid State Mater. Sci. **24**, 1 (1999).
[38] T. Laurila and J. Molarius, Crit. Rev. Solid State Mater. Sci. **28**, 185 (2003).
[39] W. Feng, D. D. Dung, Y. Shin, D. V. Thiet, and S. Cho, J. Korean Phys. Soc. **56**, 1382 (2010).